RESEARCH ARTICLE
DOI: 10.54926/jnamt.2024.1516922
J Nav Architect Mar Technol 2024;226(2):1-11

Non-Linear Numeric Parametric Roll Analysis for the DTMB 5512 in Regular Waves

Fikret Dündar, Ferdi Çakıcı

Department of Naval Architecture and Marine Engineering, Faculty of Marine Sciences, Yıldız Technical University, İstanbul, Türkiye

To cite this article: F. Dündar, and F. Çakıcı. Non-linear numeric parametric roll analysis for the DTMB 5512 in regular waves. *J Nav Architect Mar Technol*. 2024;226(2):1-11.

Received: 16.07.2024 - **Revised:** 29.10.2024 - **Accepted:** 30.10.2024 - **Publication Date:** 31.01.2025

Abstract

Parametric roll motion is a phenomenon that occurs within seconds, and it can reach high roll degrees. If the periodic stability of a ship changes, it may cause roll angles over 25 degrees, threatening the safety of the crew and the ship. This also threatens the operational skills of the ship. To investigate this phenomenon, a navy combatant model DTMB 5512 is selected. The model also has a bilge keel. Himeno's method was employed to calculate damping coefficients based on roll decay experiments (from literature) conducted at various model speeds and initial angles. This approach facilitated the extraction of both linear and non-linear damping coefficients from experimental data. Additionally, extinction coefficients were also obtained. Maxsurf stability software was utilized to compute *GM* values and generate the *GZ* curve. A Runge-Kutta method implementation in Python programming enabled numerical analysis, comprising a total of 240 simulations across 10 wave heights and 24-speed scenarios. For each scenario, the maximum roll angle was determined. It was observed that roll angles increased notably when the encounter frequency approached twice the natural roll frequency. Based on the analysis findings, maximum roll angles did not exceed 25 degrees, indicating that the DTMB 5512 model is not vulnerable to parametric roll resonance.

Keywords: DTMB 5512, parametric roll resonance, damping, roll decay

1. Introduction

Parametric roll motion is a rapid phenomenon characterized by high roll angles (exceeding 25 degrees) occurring within seconds. Research on parametric roll began in the 1930s, marked by seminal theoretical analyses by Watanabe [1] and Kempf [2]. Subsequent studies integrated nonlinear damping and Mathieu-type equations, notably by Kerwin [3] and Paulling and Rosenberg [4]. Experimental investigations by Paulling [5] in 1972 further contributed to understanding this phenomenon. The practical significance of parametric roll gained prominence in the 1990s following accidents, such as the damage to a post-panamax C11 type cargo ship in 1998, which prompted detailed publications emphasizing its importance [6]. Bulian [7] explored the nonlinear damped 1-degree-of-freedom motion associated with the parametric roll. The International Maritime Organization (IMO) included parametric roll in the second-generation stability criteria for ship safety [8], while recent studies continue to investigate various aspects of parametric roll [9,10,11]. Parametric roll analysis plays a critical role in maritime safety guidelines established by classification societies such as ClassNK [12] and ABS [13], as well as the updated guidelines from the IMO in 2020 [14]. The metacentric height (*GM*) is a pivotal factor in parametric roll analysis,

Address for Correspondence: Ferdi Çakıcı, Department of Naval Architecture and Marine Engineering, Faculty of Marine Sciences, Yıldız Technical University, İstanbul, Türkiye
E-mail: fcakici@yildiz.edu.tr
ORCID ID: orcid.org/0000-0001-9752-1125

varying with different loading conditions. Recent research has also explored computational fluid dynamics solutions tailored to specific vessel types, including fishing boats [15].

In this study, we conducted numerical parametric roll analysis for the DTMB 5512 model. Damping coefficients were derived using roll decay data specific to the DTMB 5512, as detailed by Irvine et al. [16]. Both linear and nonlinear damping coefficients were considered, adhering closely to IMO guidelines [17]. The restoring term *GZ* was modelled using a seventh-degree equation, while *GM* was approximated using a cosine function. The numerical analysis was executed utilizing the Runge-Kutta method.

2. Physical Background

Parametric roll can occur when the ship length and the wavelength of encountered waves are closely aligned, and the wave encounter frequency is twice the ship natural roll frequency. Changes in transverse inertia in the head or following seas lead to fluctuations in *GM* (metacentric height).

Ships typically have a wider beam at upper decks, especially in cargo ships, where the underwater portion is streamlined compared to the above-water structure. Consequently, when the wave trough is amidships, the ship experiences greater inertia, enhancing its stability. Conversely, when the wave crest is amidships, the ship encounters less inertia, resulting in decreased stability. The variation in *GM* mentioned above is influenced by factors such as wavelength, wave height, and the wave position. Figures 1 and 2 illustrate the submerged portions of the ship at different wave positions.

Figures 3 and 4 depict the submerged waterplane area of the ship at various positions relative to the wave. These perspectives should be considered together for a comprehensive evaluation. As the wave moves past the ship, the relationship with width becomes crucial, significantly as the height varies at different points along the ship.

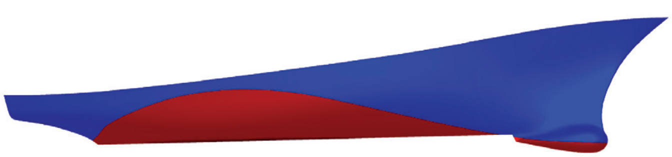

Figure 1. View of the DTMB 5512 when the ship is on the wave crest.

Figure 2. View of the DTMB 5512 when the ship is on the wave trough.

The variation of these two variables relative to the wave's position defines the changes in *GM*.

Parametric roll is characterized by periodic changes influenced by the relationship between the ship's natural roll frequency and the encounter frequency of waves. Figure 5 illustrates a scenario where the encounter frequency is twice the ship's natural roll frequency. Initially, at the zero-roll degree point with the wave crest position, the ship experiences zero roll angle. As the wave progresses, the ship reaches its maximum roll angle with the wave in a trough position. The ship's stability is enhanced during this phase due to a greater restoring moment. Subsequently, as the ship continues to roll, the wave position returns to a crest. At this stage, the ship's stability decreases, leading to increased rolling compared to earlier stages, the ship reaches its maximum roll angle again when the wave returns to a trough position. Consequently, stability improves once more. This cyclic pattern of roll and stability changes is characteristic

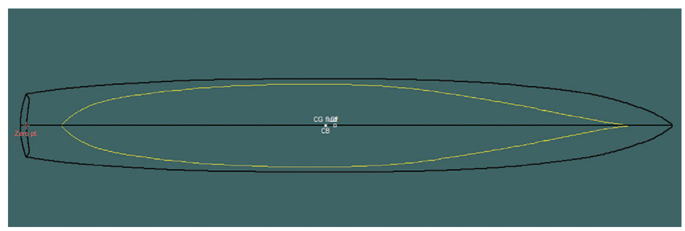

Figure 3. Waterplane area view of the DTMB 5512 when the ship is on the wave crest.

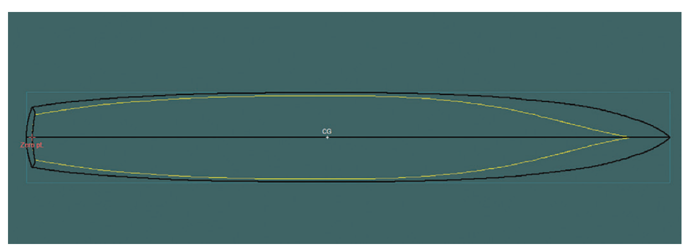

Figure 4. Waterplane area view of the DTMB 5512 when the ship is on the wave trough.

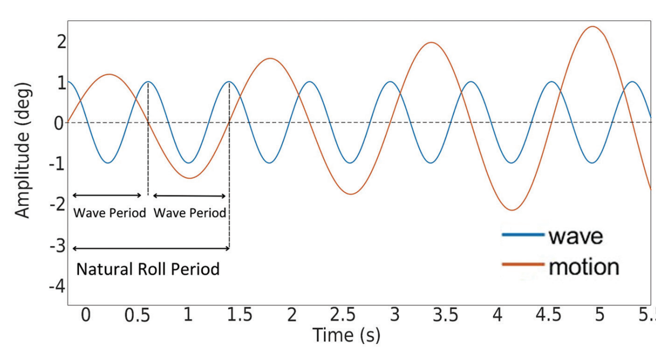

Figure 5. Sample wave profile (x-axis is time in seconds, y-axis is motion in degrees).

of parametric roll phenomena, influenced by the dynamic interplay between wave conditions and the ship's response.

According to Luthy [11], the following conditions are required for parametric roll to occur:

- Wavelength should be close to the length of the ship,
- *GM* value should be affected as much as possible by the interaction of the hull of the ship with the wave profile,
- Encounter frequency should be twice the natural roll frequency of the ship,
- Head or following seas,
- Insufficient damping.

3. The Method of Analysis

3.1. General Information About Analysis

The main parameters of DTMB 5512 (Iowa scale) is given in Table 1 [16].

In many studies, observing different *GM* values for DTMB 5512 is possible. The reason of the difference is caused by the baseline selection. In this study, Figure 6 is used as the baseline, representing the lowest point of the sonar dome.

The equation of roll motion can be found in various forms in the literature. As a basis, the Mathieu-type (the changing *GM* in time) in Equation 1 can be used if the ship is sailing in longitudinal seas and there is no wave roll moment:

$$\left(I_{44}+A_{44}\right)\ddot{\phi}+B_{44}\dot{\phi}+\Delta GM(t)\phi \;=\; 0 \tag{1}$$

Here B_{44} is the linear or linearized damping coefficient and $\Delta GM(t)\phi$ is the linear restoring moment. These linear terms can be used at the lower roll degrees, but parametric roll resonance reaches high roll degrees, and this formula can not be used in this situation. Also, the Mathieu equation can only indicate whether parametric rolling starts or not. At higher roll degrees, the solution goes to infinite. Therefore, the Mathieu equation is insufficient to find the final degree of parametric roll resonance. Therefore, a non-linear equation can be used to better express the dynamics at higher roll degrees. After introducing the non-linear terms, the Equation 2 becomes the following:

$$\left(I_{44}+A_{44}\right)\ddot{\phi}+B_{44L}\dot{\phi}+B_{44NL}\dot{\phi}^{3}+\Delta GZ(\phi,t) \;=\; 0 \tag{2}$$

3.2. Restoring Term

$$GZ(\phi,t) \;=\left[GM_{m}+GM_{a}cos(\omega_{e}\;\;t)\right]\left[a\phi^{7}+b\phi^{5}+c\phi^{3}+d\phi\right] \tag{3}$$

The restoring term is expressed as Equation 3 [9]. As seen, *GZ* is a function that has different parameters. GM_{max} and GM_{min} are maximal and minimal instantaneous values of *GM* for several wave crest positions along the ship hull as stated in Belenky et al., [18].

$$GM_{m} \;=\; 0.5\left(GM_{max}+GM_{min}\right) \tag{4}$$

$$GM_{a} \;=\; 0.5\left(GM_{max}-GM_{min}\right) \tag{5}$$

Also, wave height is defined as follows :

$h_j \;=\; 0.01\ jL\ ,\ \text{where } j \;=\; 0,1,2,3\ldots9,10$

Table 2 shows GM_m and GM_a values for different wave heights calculated with the help of the Maxsurf Stability [19]. The wave heights listed in the Table 2 are 0.065 meters less than the actual values. This is because the baseline has been chosen as the reference point. The distance of 0.065 meters is the gap between the baseline and the orange line seen in Figure 6.

Table 1. Ship data of DTMB 5512.

Symbol	Unit	Value
L_{PP}	m	3.048
L_{WL}	m	3.052
B_{WL}	m	0.409
C_B	-	0.506
T	m	0.132
Displacement force	N	843.66
KG	m	0.163
GM	m	0.043
$\lambda_w = L_{WL}$	m	3.052

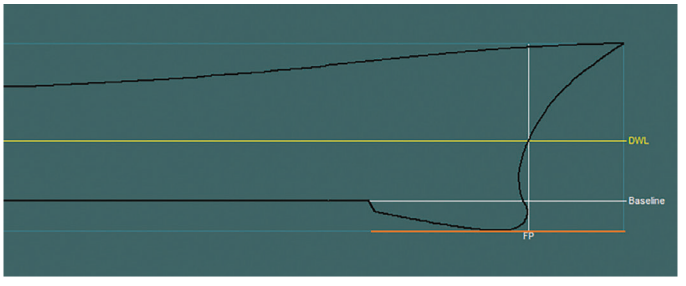

Figure 6. Baseline selection

Table 2. GM_m, GM_a and wave height values.

H (m)	**0.024**	**0.048**	**0.072**	**0.096**	**0.120**	**0.144**	**0.168**	**0.192**	**0.216**	**0.240**
GM_a (m)	0.0025	0.0050	0.0065	0.0085	0.0100	0.0120	0.0140	0.0155	0.0180	0.0185
GM_m (m)	0.0425	0.0420	0.0415	0.0425	0.0430	0.0440	0.0450	0.0465	0.0480	0.0485

To make it easier to express the GM changing with the position of the wave, the encounter frequency and time are used. An example result is shown in Figure 7. The curves in Figure 7, are calculated for DTMB 5512 and show an example cosine approximation for DTMB 5512.

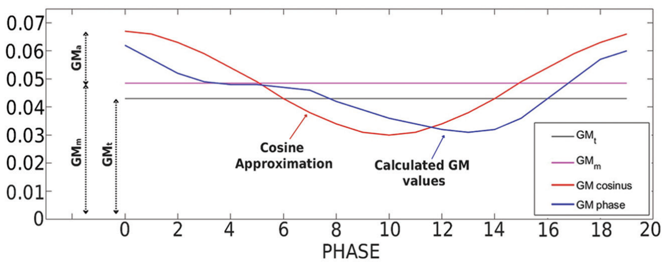

Figure 7. Cosine function of GM values.

To find a, b, c, and d coefficients, the GZ (Restoring moment arm) graph was obtained with the help of the Maxsurf Stability software. Then GZ values were divided by GM_T value. Using Matlab, a curve was fitted for GZ/GM_T values by the form in Equation 3. The fitted curve can be seen in Figure 8. The a, b, c, and d coefficients obtained as a result of curve fitting are as in Table 3.

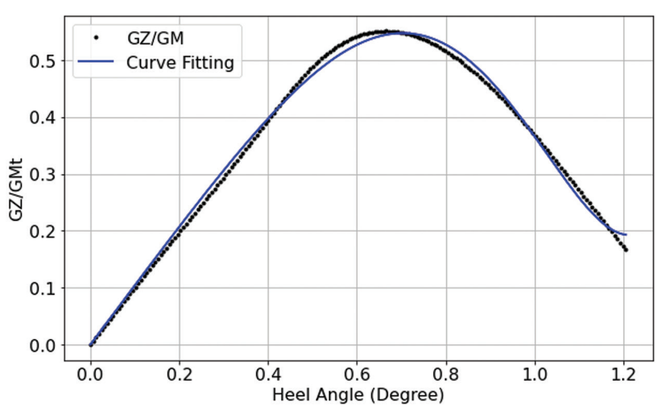

Figure 8. GZ curve fitting.

3.3. Mass Moment of Inertia and Hydrodynamic Added Inertia

As stated in Equation 6, a restoring term and model natural roll period are needed to find inertia and added inertia. The restoring term was calculated with the help of Equation 7. When the roll decay results of the model are examined, different natural roll periods are observed at various speeds and initial angles. The natural roll period was calculated at all speeds and initial angles. Table 4 shows a natural roll period with the average of these values was obtained.

Table 3. GZ coefficients.

Symbol	Value
a	0.4518
b	-0.9550
c	-0.1745
d	1.0440

$$T_\phi = 2\pi\sqrt{\frac{I_{44}+A_{44}}{C_{44}}} \tag{6}$$

$$C_{44} = \Delta\ GM \tag{7}$$

Table 4. Froude numbers, initial angles, and natural roll periods (s).

Fn	10 Degree	15 Degree	20 Degree	Mean
0.069	1.610	1.616	1.629	1.618
0.096	1.615	1.621	1.622	1.619
0.138	1.613	1.615	1.617	1.615
0.190	1.599	1.603	1.609	1.604
0.280	1.579	1.585	1.583	1.582
0.340	1.550	1.559	1.562	1.557
0.410	1.531	1.520	1.543	1.531
			Total mean:	1.590

The average inertia of the ship was found using the average natural period and restoring term.

$$I_{44} + A_{44} = 2.322\ \ kg\ \ m^2$$

3.4. Coefficients of Non-linear Representation of Roll Damping

Equation 8 is the general formula for the nonlinear damping coefficients. In this study, the B_2 term will be ignored since the quadratic damping coefficient will not be used. In the rest of the study, B_L stands for B_1 as it represents the linear coefficient of roll damping and B_{NL} stands for the B_3 as cubic coefficient of roll damping.

$$\Delta\phi = \frac{\pi\omega_\phi}{2C_{44}}\phi_m\left[B_1 + \frac{8}{3\pi}\omega_\phi\phi_m B_2 + \frac{3}{4}\omega_\phi^2\phi_m^2 B_3\right] \tag{8}$$

To determine the damping coefficients, roll decay test data were analyzed across all speeds and initial angles of 10°, 15°, and 20°. Given the intention to incorporate coefficients of non-linear representation of roll damping in the study, Himeno's method [20] was employed. This method is suited explicitly for extracting non-linear damping characteristics from experimental data, ensuring accurate characterization of the ship's damping behavior during roll decay tests. In experimental data, as in Figure 9, the red points where the roll degree of the model peaks are determined. Using Equations 9 and 10, the difference between the peak points and, after that, the averages of the peak points are calculated (Table 5).

$$\Delta\phi = \phi_{n-1} - \phi_n \quad (9)$$

$$\phi_m = \frac{\phi_{n-1} + \phi_n}{2} \quad (10)$$

After calculating ϕ_m and $\Delta\phi$ values, a curve fitting was performed using Matlab software. In Figure 10, the curve fitting using peak values can be seen. With the equation obtained with the curve, Equation 8 can be equated. This can be seen in Equation 11. The transformation in Equation 7 is used for the restoring term (C_{44}). With the modifications made to the Equation 11, and B_L, B_{NL} are obtained in Equation 12 and Equation 13.

The process in Figure 10 was performed for each speed and initial angle. Table 6 shows the values of k_1 and k_3.

$$k_1\phi_m + k_3\phi_m^3 = \frac{\pi}{2}\frac{\omega_\phi}{C_{44}}\phi_m B_L + \frac{\pi}{2}\frac{\omega_\phi}{C_{44}}\phi_m \frac{3}{4}\omega_\phi^2\phi_m^2 B_{NL} \quad (11)$$

$$B_L = \frac{(2\,k_1\,\Delta GM)}{\pi\omega_\phi} \quad (12)$$

$$B_{NL} = \frac{(8k_3\,\Delta GM)}{3\pi\omega_\phi^3} \quad (13)$$

The relation of the extinction coefficients can be seen in Equation 14 and 15. "a and c" are called the decay coefficients (obtained from free-roll test). In our equation, they correspond to k_1, k_3. With the help of this equation, the relation between ship speed and extinction coefficients can be seen in Table 7.

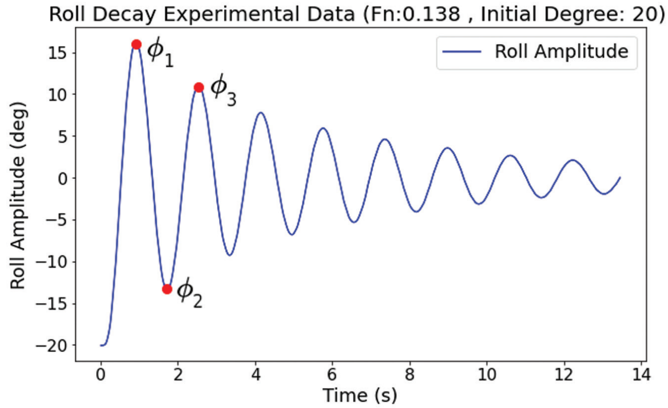

Figure 9. Roll decay curve.

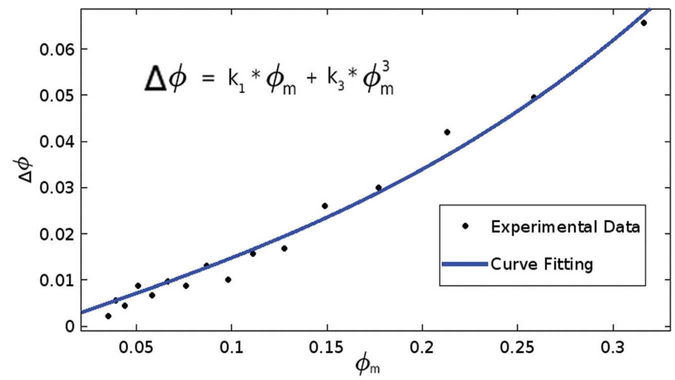

Figure 10. Curve fitting ϕ_m - $\Delta\phi$.

Table 5. An example of peaks determination (Fn: 0.138, initial degree: 20).

i	0	1	2	3	4	5	6	7	8	9	10
Degree	-20.000	16.243	-13.403	10.997	-9.276	7.781	-6.817	5.919	-5.342	4.591	-4.093
Radian	-0.349	0.283	-0.234	0.192	-0.162	0.136	-0.119	0.103	-0.093	0.080	-0.071
ϕ_m	0.316	0.259	0.213	0.177	0.149	0.127	0.111	0.098	0.087	0.076	0.067
$\Delta\phi$	0.066	0.050	0.042	0.030	0.026	0.017	0.016	0.010	0.013	0.009	0.010

Table 6. Froude numbers with k_1 and k_3, B_L and B_{NL} values.

	10 Degrees		15 Degrees		20 Degrees		Mean		Mean	
Fn	k_1	k_3	k_1	k_3	k_1	k_3	k_1	k_3	B_{NL}	B_L
0.069	0.0852	0.7934	0.0925	0.6461	0.0964	0.6273	0.0914	0.6889	0.3124	0.5172
0.096	0.0735	2.4241	0.0865	1.2270	0.0885	1.0079	0.0828	1.5530	0.7041	0.4689
0.138	0.1231	2.3301	0.1266	1.4163	0.1316	1.0453	0.1271	1.5972	0.7242	0.7195
0.190	0.1888	-0.1952	0.1821	0.6285	0.1814	0.6407	0.1841	0.3580	0.1623	1.0421
0.280	0.1912	2.8576	0.2042	1.3570	0.2220	0.4862	0.2058	1.5669	0.7104	1.1649
0.340	0.2178	2.8760	0.2292	1.4073	0.2403	0.8342	0.2291	1.7058	0.7734	1.2968
0.410	0.2980	0.4669	0.2926	0.9056	0.2971	0.4596	0.2959	0.6107	0.2769	1.6750

Table 7. Extinction coefficients.

Fn	γ	κ_a
0.069	470.5244	0.0582
0.096	1060.661	0.0527
0.138	1090.871	0.0809
0.190	244.5051	0.1172
0.280	1070.177	0.1310
0.340	1165.042	0.1458
0.410	417.0930	0.1884

The relationship between decay coefficients, coefficients of the non-linear representation of roll damping, and extinction coefficients can be examined in detail in the ITTC documents [21].

$$a = \frac{\pi}{2}\frac{2\alpha}{\omega_\phi} = \frac{\pi}{2}\kappa_a \tag{14}$$

$$c\left(\frac{180}{\pi}\right)^2 = \frac{3\pi}{8}\omega_\phi \gamma \tag{15}$$

After these calculations, a scatter plot was drawn with speed on the x-axis and linear (B_L) or non-linear (B_{NL}) damping coefficients on the y-axis. As can be seen in Figures 11 and 12, a 2nd order curve fitting was performed for the linear coefficient, while a 1st order curve fitting was performed for the non-linear damping coefficient. Thus, the relationship between the damping coefficients and the forward speed was revealed for DTMB 5512.

3.5. Numerical Analysis Background

Runge-Kutta method was used for numerical analysis. The code was written in Python language to perform the analysis. The algorithm can be seen in Figure 13. The inputs of the algorithm are as follows:

- Speed

Since the ship will be examined with the head and the following waves, therefore $\cos(\varphi_w) = 1$ or $\cos(\varphi_w) = -1$, respectively.

$$\omega_e = \omega - k\,V\cos(\varphi_w) \tag{16}$$

Equation 16 shows how the encounter frequency is calculated for the speed the ship has. φ_w refers to the angle of encounter. Therefore, in Table 8, $i \leq 12$ refers to following waves, while $i > 12$ refers to head waves. The speed coefficients in the table express the ratio with service speed. The service speed of the ship is assumed to be Fn= 0.41. With the help of Equation 17, the ship's service speed at Fn= 0.41 is equal to 2.2434 (m/s).

$$Fn = \frac{V}{\sqrt{g\ L}}$$
$$V_s = 2.2434\ m/s \tag{17}$$

- Wave height

Wave height as an input determines the values of GM_m and GM_a in the equation. More information on wave heights is in section 3.2.

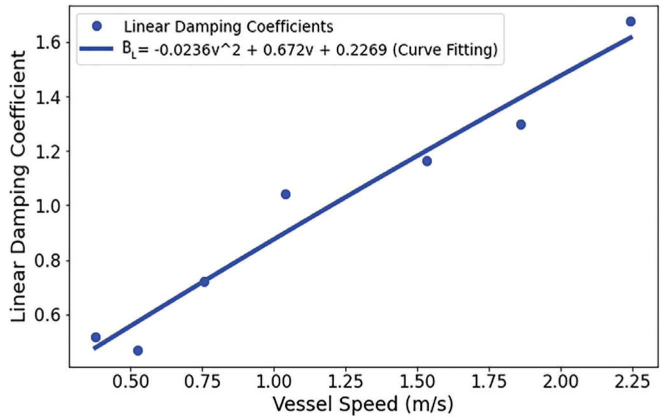

Figure 11. Linear coefficient - ship speed (m/s).

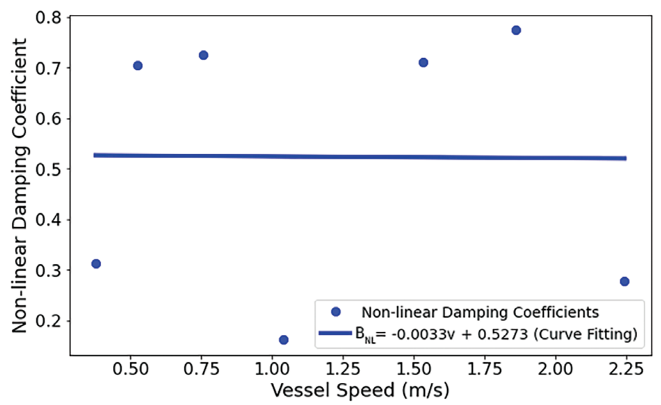

Figure 12. Non-linear coefficient - ship speed (m/s).

Table 8. Speed coefficients.

i	k_i	i	k_i
1	1.000	13	-1.000
2	0.991	14	-0.991
3	0.996	15	-0.996
4	0.924	16	-0.924
5	0.866	17	-0.866
6	0.793	18	-0.793
7	0.707	19	-0.707
8	0.609	20	-0.609
9	0.500	21	-0.500
10	0.383	22	-0.383
11	0.259	23	-0.259
12	0.131	24	-0.131

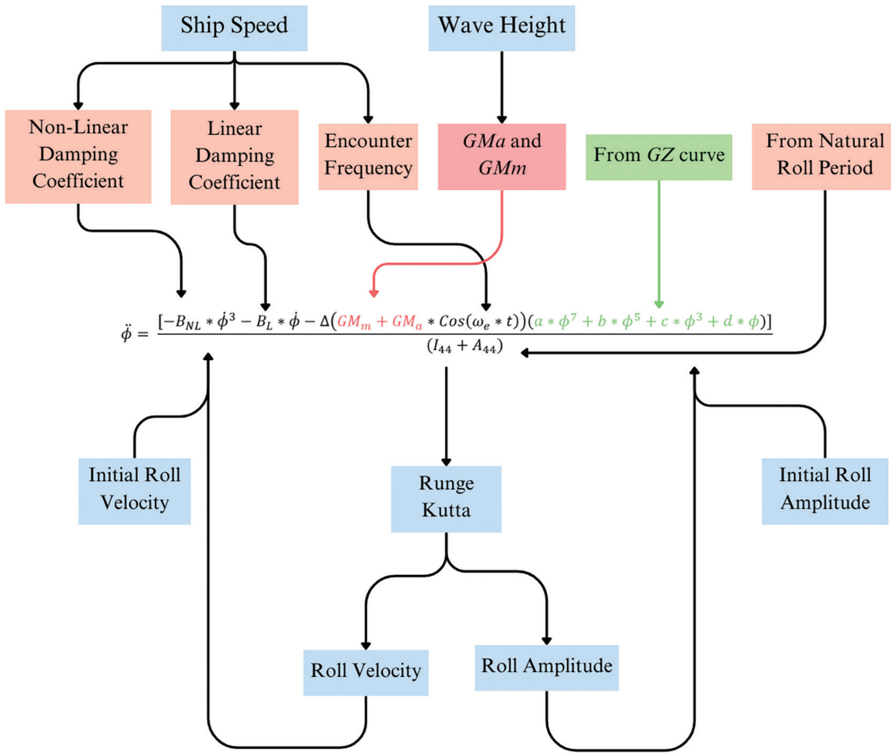

Figure 13. Algorithm of analysis.

- Initial roll amplitude and roll velocity

The initial roll angle and roll velocity for the analysis are as follows:

$\phi(0) = 0.0872\ rd\ (5\text{deg})$

$\dot{\phi}(0) = 0\ rd/s$

- Time

The time interval for numerical analysis was determined as 0.01 seconds.

- Runge-Kutta Method

In the numerical analysis, the 4th-order Runge-Kutta method was used to calculate the instantaneous roll angles and velocities.

4. Results and Discussion

4.1. Validation

The experimental results were compared with those derived from the Runge-Kutta method to assess the proximity of the calculated damping coefficients to experimental values [16]. The equation was structured to depict free-damped motion. The numerical analysis using the Runge-Kutta method was conducted for different initial roll angles and vessel speeds. Figures 14 to 21 show that the numerical results closely match the experimental data obtained under the same initial conditions. This agreement between experimental and numerical results shows that the coded Runge Kutta method gives reliable outcomes.

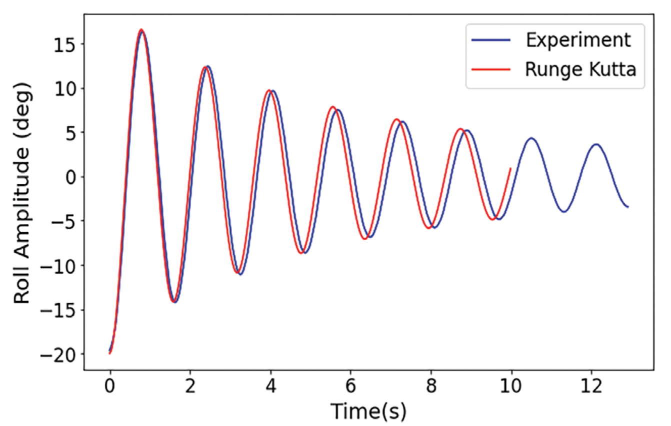

Figure 14. Roll amplitude at Fn=0.069 and initial roll angle=20.

4.2. Results

Table 9 on the subsequent pages displays the wave heights, ship speeds, encounter frequencies, and maximum roll angles (degrees). Additionally, motion graphs depicting these unstable states can be found in from Figure 21 to Figure 26. Please note that following figures show the head sea cases.

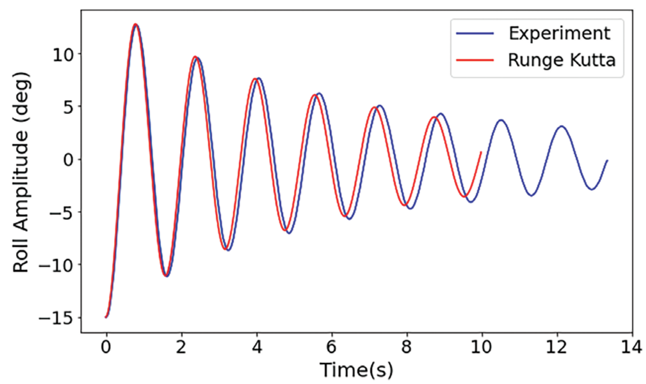

Figure 15. Roll amplitude at Fn=0.096 and initial roll angle=15.

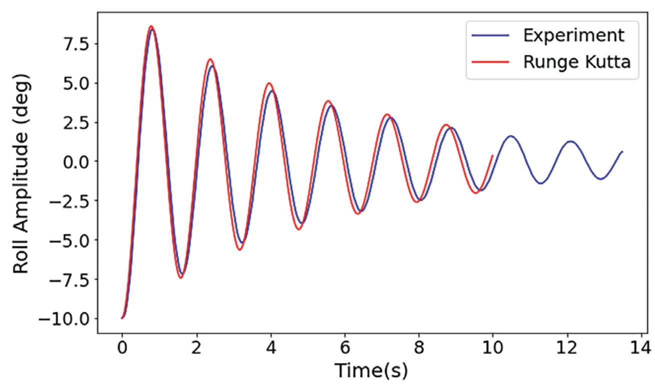

Figure 16. Roll amplitude at Fn=0.138 and initial roll angle=10.

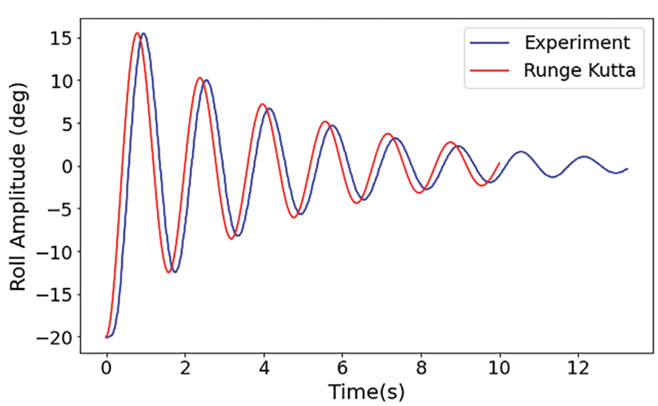

Figure 17. Roll amplitude at Fn=0.190 and initial roll angle=20.

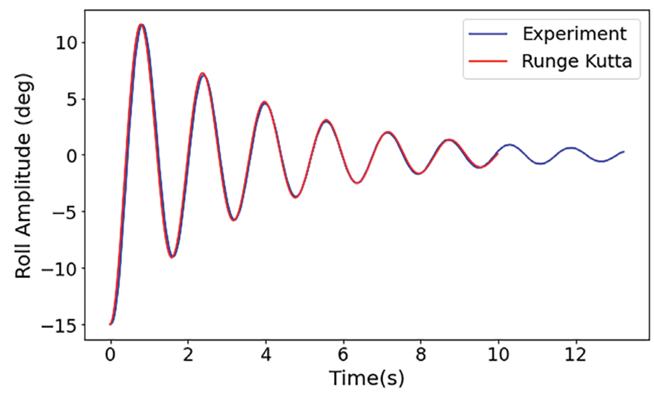

Figure 18. Roll amplitude at Fn=0.280 and initial roll angle=15.

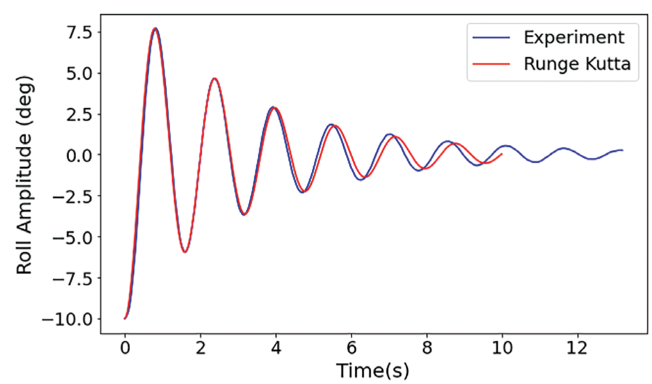

Figure 19. Roll amplitude at Fn=0.340 and initial roll angle=10.

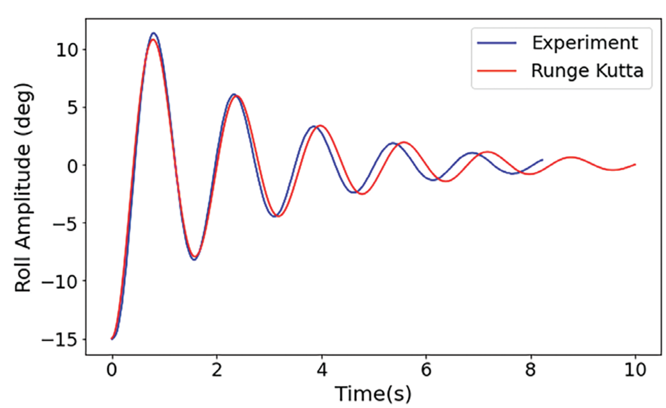

Figure 20. Roll amplitude at Fn=0.410 and initial roll angle=15.

Table 9. Maximum roll angle.

H (m) / Fn (-)	0.024	0.048	0.072	0.096	0.120	0.144	0.168	0.192	0.216	0.240	ω_e	ω_e / ω_Φ
0.054	5.00	5.00	5.00	4.99	4.99	4.99	4.99	4.99	4.99	4.99	3.89	0.865
0.106	5.00	5.00	5.00	4.99	4.99	4.99	4.99	4.99	4.99	4.99	3.30	0.734
0.157	5.00	5.00	5.00	4.99	4.99	4.99	4.99	4.99	4.99	4.99	2.73	0.606
0.205	5.00	5.00	5.00	4.99	4.99	4.99	4.99	4.99	4.99	4.99	2.18	0.486
0.250	5.00	5.00	5.00	4.99	4.99	4.99	4.99	4.99	4.99	4.99	1.68	0.374
0.290	5.00	5.00	5.00	4.99	4.99	4.99	4.99	4.99	4.99	4.99	1.23	0.273
0.325	5.00	5.00	5.00	4.99	4.99	4.99	4.99	4.99	4.99	4.99	0.83	0.185
0.355	5.00	5.00	5.00	4.99	4.99	4.99	4.99	4.99	4.99	4.99	0.49	0.110
0.379	5.00	5.00	5.00	4.99	4.99	4.99	4.99	4.99	4.99	4.99	0.23	0.050
0.396	5.00	5.00	5.00	4.99	4.99	4.99	4.99	4.99	4.99	4.99	0.03	0.007
0.406	5.00	5.00	5.00	4.99	4.99	4.99	4.99	4.99	4.99	4.99	-0.08	0.018
0.410	5.00	5.00	5.00	4.99	4.99	4.99	4.99	4.99	4.99	4.99	-0.12	0.028
0.054	5.00	5.00	5.00	4.99	4.99	4.99	5.09	5.11	5.21	5.21	5.10	1.135
0.106	5.00	5.00	5.00	4.99	5.01	5.18	5.33	5.37	5.51	5.52	5.69	1.266
0.157	5.00	5.00	5.00	4.99	5.03	5.27	5.50	5.59	5.80	5.82	6.26	1.394
0.205	5.00	5.00	5.00	4.99	4.99	5.09	5.38	5.57	5.88	5.93	6.80	1.514
0.250	5.00	5.00	5.00	4.99	4.99	4.99	4.99	5.21	5.60	5.67	7.31	1.626
0.290	5.00	5.00	5.00	4.99	4.99	4.99	4.99	5.16	5.82	5.92	7.76	1.727
0.325	5.00	5.00	5.00	4.99	4.99	4.99	6.96	9.67	13.47	13.49	8.16	1.815
0.355	5.00	5.00	5.00	4.99	4.99	4.99	4.99	6.75	13.68	14.45	8.49	1.890
0.379	5.00	5.00	5.00	4.99	4.99	4.99	4.99	4.99	8.63	10.70	8.76	1.950
0.396	5.00	5.00	5.00	4.99	4.99	4.99	4.99	4.99	4.99	4.99	8.96	1.993
0.406	5.00	5.00	5.00	4.99	4.99	4.99	4.99	4.99	4.99	4.99	9.07	2.018
0.410	5.00	5.00	5.00	4.99	4.99	4.99	4.99	4.99	4.99	4.99	9.11	2.028

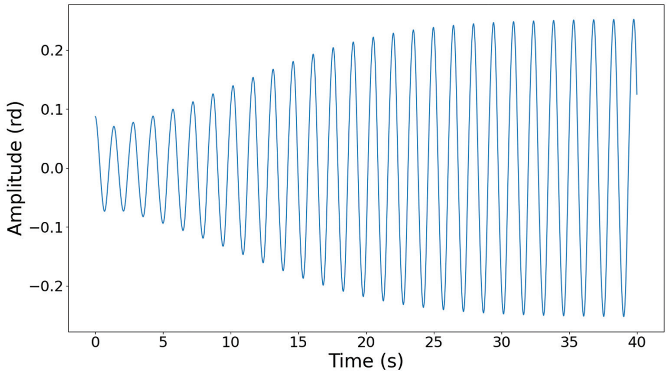

Figure 21. Speed: 1.943 m/s - wave height: 0.240 m.

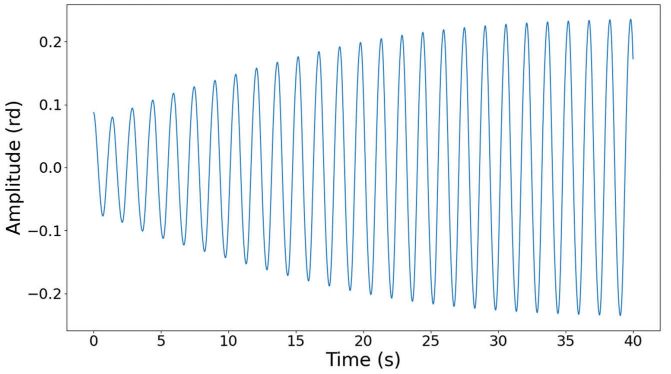

Figure 22. Speed: 1.7789 m/s - wave height: 0.240 m.

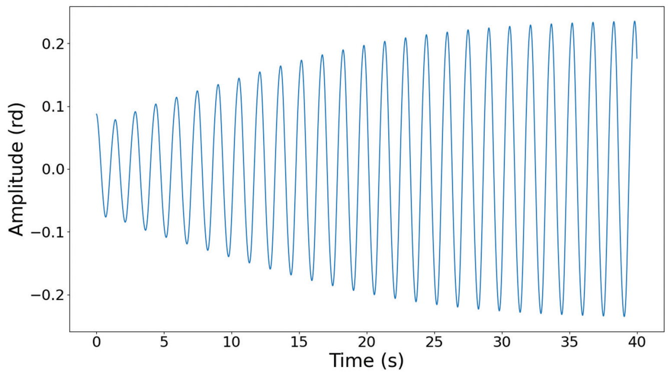

Figure 23. Speed: 1.7789 m/s - wave height: 0.216 m.

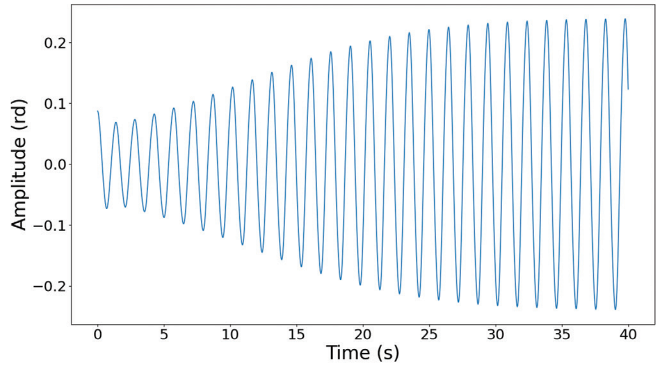

Figure 24. Speed: 1.943 m/s - wave height: 0.216 m.

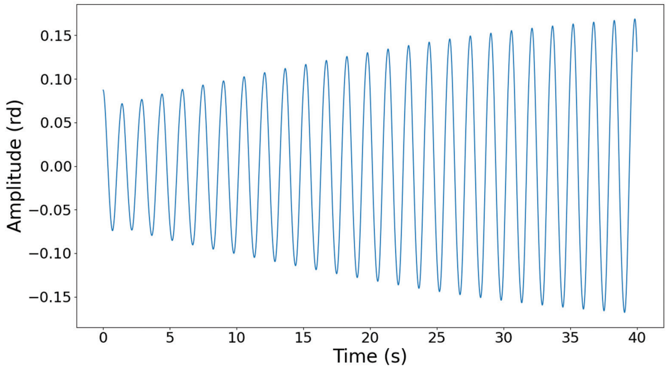

Figure 25. Speed: 1.7789 m/s - wave height: 0.192 m.

5. Conclusion

Parametric roll resonance significantly impacts the operational capabilities of naval combatants. Therefore, in the current study, an analysis of parametric roll resonance was conducted for the DTMB 5512 model. This analysis involved determining both linear and non-linear damping coefficients, as well as extinction coefficients. *GM* values for the restoring term were established based on varying wave

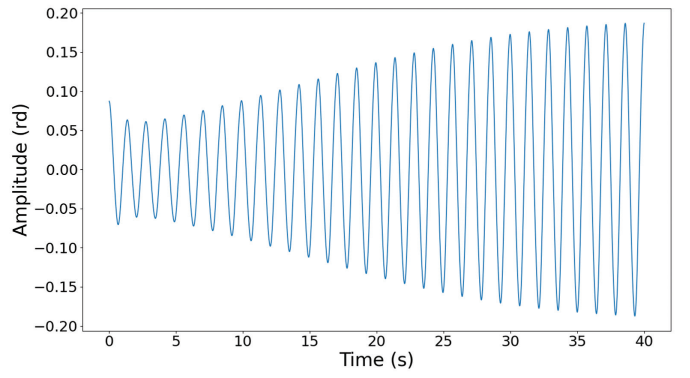

Figure 26. Speed: 2.0727 m/s - wave height: 0.240 m.

heights, and coefficients of *GZ* were also calculated. Using the Runge-Kutta method for analysis, maximum roll angles were observed to reach approximately 14 degrees. Although this angle does not meet the IMO threshold of 25 degrees for considering parametric roll, it is crucial to recognize that such roll angles still pose significant risks and should be carefully evaluated.

NOMENCLATURE

L_{PP} : Length between perpendiculars

L_{WL}: Length of waterline

B_{WL}: Maximum moulded breadth at design waterline

C_B: Block coefficient

T: Draught

KG: Centre of gravity above moulded base or keel

GM: Transverse metacentric height

λ_w: Wave length

Fn: Froude Number

ω_e: Encounter frequency

ω_ϕ : Natural roll frequency

Acknowledgements

This study is supported by project number 123M482 of the Scientific and Technological Research Council of Türkiye (Tübitak).

Footnotes

Authorship Contributions

Concept: F. Dündar, and F. Çakıcı., Design: F. Dündar, and F. Çakıcı., Data Collection or Processing: F. Dündar, and F. Çakıcı., Analysis or Interpretation: F. Dündar, and F. Çakıcı., Literature Search: F. Dündar, and F. Çakıcı., Writing: F. Dündar, and F. Çakıcı.

Conflict of Interest: No conflict of interest was declared by the authors.

Financial Disclosure: The authors declared that this study received no financial support.

6. References

[1] Y. Watanabe, "On the dynamic properties of the transverse instability of a ship due to pitching," *Journal of the Society of Naval Architects of Japan*, vol. 53, pp. 51-70, 1934.

[2] G. Kempf, "Die Stabilität Beanspruchung der Schiffe durch Wellen und Schwingungen," *Werft Reederei Hafen*, vol. 19, pp. 200-202, 1938.

[3] J. E. Kerwin, "Note on rolling in longitudinal waves," *International Shipbuilding Progress*, vol. 2, no. 16, pp. 597-614, 1955.

[4] J. R. Paulling and R. M. Rosenberg, "On unstable ship motions resulting from nonlinear coupling," *Journal of Ship Research*, vol. 3, pp. 36-46, 1959.

[5] J. R. Paulling, S. Kastner, and S. Schaffran, "*Experimental studies of capsizing of intact ships in heavy seas*," U.S. Coast Guard Technical Report (also IMO Doc. STAB/7), 1972.

[6] W. L. France, et al., "An investigation of head-sea parametric rolling and its influence on container lashing systems," *Marine Technology*, vol. 40, no. 1, 2003.

[7] G. Bulian, "Approximate analytical response curve for a parametrically excited highly nonlinear 1-DOF system with an application to ship roll motion prediction," *Nonlinear Analysis: Real-World Applications*, vol. 5, no. 4, pp. 725-748, 2004.

[8] N. Umeda, "Current status of second generation intact stability criteria," *Proceedings of the 13th International Ship Stability Workshop*, Brest, pp. 138-157, 2013.

[9] F. Cakici, "A numerical application of ship parametric roll under second generation stability criteria," *Journal of ETA Maritime Science*, vol. 7, no. 3, pp. 242-251, 2019.

[10] H. I. Çopuroğlu, E. Pesman, and M. Taylan, "Assessment of second-generation intact stability criteria and case study for a Ro-Ro ship," *Proceedings of the 19th International Ship Stability Workshop*, Istanbul, Turkiye, 9-11 Sept. 2023, pp. 315-320.

[11] V. Luthy, "Probability of occurrence of parametric roll on a predefined sea state," PhD thesis, HESAM, Paris, 2023.

[12] ClassNK, "Guidelines on preventive measures against parametric rolling (Edition 1.0)," ClassNK, 2023.

[13] ABS, "The assessment of parametric roll resonance in the design of container carriers," 2019.

[14] IMO, "Interim guidelines on the second generation intact stability criteria," International Maritime Organization, London, UK, 2020.

[15] M. Iqbal, et al., "Unsteady RANS CFD simulation on the parametric roll of small fishing boat under different loading conditions," *J. Marine. Sci. Appl.*, vol. 23, pp. 327-351, 2024.

[16] M. Irvine, J. Longo, and F. Stern, "Towing tank tests for surface combatant for free roll decay and coupled pitch and heave motions," in *Proceedings of the 25th ONR Symposium on Naval Hydrodynamics*, St Johns, Canada, 2004.

[17] International Towing Tank Conference (ITTC), "Estimation of roll damping," ITTC Recommended Procedures and Guidelines, 7.5-02-07-04.5, 2021.

[18] V. Belenky, C. Bassler, and K. Spyrou, "Development of second generation intact stability criteria," Hydromechanics Department Report, Naval Surface Warfare Center Carderock Division-50-TR-2011/065, 2011.

[19] Maxsurf Stability, "Windows Version 20 User Manual."

[20] Y. Himeno, "Prediction of ship roll damping: A state of the art," Report No. 239, Department of Naval Architecture and Marine Engineering, The University of Michigan, Ann Arbor, MI, 1981.

[21] International Towing Tank Conference (ITTC), "Numerical Estimation of Roll Damping," ITTC Recommended Procedures and Guidelines, 7.5-02-07-04.5, 2011.